Proceedings World Geothermal Congress 2023
Beijing, China, 9-11 October, 2023

Structural and geothermal field assessment at Ytri-Vík, North Iceland

Anett Blischke[1], Arnar Már Vilhjálmsson[1], Sigurveig Árnadóttir[1], Egill Árni Gudnason[2], Hörður Tryggvasson[3], Unnur Þorsteinsdóttir[4], Albert Þorbergsson[5], Þorbjörg Ágústsdóttir[2], Gunnlaugur M. Einarsson[5], Finnbogi Óskarsson[2], Ólafur G. Flóvenz[2], and Bjarni Gautason[1]

[1] Iceland GeoSurvey, Branch at Akureyri, Rangárvöllum, 603 Akureyri, Iceland

[2] Iceland GeoSurvey, Urðarhvarfi 8, 203 Kópavogur, Iceland

[3] Norðurorka - Utility Company of Akureyri and Eyjafjördur, Rangárvellir, 603 Akureyri, Iceland

[4] EFLA Consulting Engineers, Glerárgötu 32 9, 600 Akureyri, Iceland

[5] National Planning Agency of Iceland, Borgartún 7b, 105 Reykjavík, Iceland

E-mail: anb@isor.is; arnar.mar.vilhjalmsson@isor.is, sigurveig.arnadottir@isor.is, egill.arni.gudnason@isor.is, hordur.h.tryggvason@no.is, unnur.thorsteinsdottir@efla.is, albert.thorbergsson@skipulag.is, thorbjorg.agustsdottir@isor.is, gme@isor.is, finnbogi.oskarsson@isor.is, oflovenz@gmail.com, bg@isor.is

Keywords: Structural geology, dike swarm, geothermal exploration, image log, high-resolution magnetic survey

ABSTRACT

Structural and geological fieldwork, drone surveying tied to borehole image data, high-resolution magnetic anomaly, geothermal water prospecting, and both regional and local seismicity data have provided a new understanding of the Ytri-Vík low-temperature geothermal field in Eyjafjördur, North Iceland. The field is located within a dike swarm system fully exposed along the coastline that is covered by younger sediments and lavas onshore and below sea level into the fjord. Delineating the extent of the geothermal field at Ytri-Vík requires a composite data analysis approach of surface and subsurface data. DJI Matrice 200 drone surveying resulted in detailed topographic and image quality of 2.8 cm resolution using the Zenmuse X4S camera that supported structural field mapping for outcrop sites along the shore at the exposed dike systems. Structural field measurements, obtained for the dike systems, fracture zones, faults, fractures, joints, mineral veins, and slickenside were summarized and compared to subsurface structural analysis data based on acoustic image logging. The primary dike systems are near-vertical and strike N-S to NNE-SSW and are linked to an active geothermal system. A second dike swarm was investigated that showed a weaker total magnetic field strength and little to no indications of surface geothermal activity and consists of NNE-SSW to NW-SE striking segments. The two dike systems correlate well with the mapped structural trends and fault zones in good agreement with magnetic anomaly trends. The primary N-S to NNE-SSW striking dikes and associated fault-fracture trends is parallel to elevated surface water conductivity indicating increased mineral contents. Associated fracturing indicates a slight left-lateral motion along fracture surfaces and NW-SE oriented stress-field orientation for $\sigma_{Hmax.}$ that is the same as indicated by direct offset earthquake locations and their fault-plane solutions. The primary dike system and the connected fracture zone is considered to be related to the main feed zone within the geothermal system at Ytri-Vík, thus enabling the up-flow of geothermal water in this area. This study underlines the necessity of combining high-resolution magnetic and drone survey data with detailed structural geological, geophysical and geochemical field studies to increase our understanding of low-temperature geothermal systems in Eyjafjördur, and within low-enthalpy areas in Iceland in general.

1. INTRODUCTION

The Ytri-Vík geothermal field, also referred to as Ytri-Haga, is located at the western shore of the Eyjafjördur fjord within North Iceland's Miocene plateau basalt region of the Tröllaskagi mountain range (Fig. 1). Here we present the preliminary results of an ongoing field study using conventional field mapping and drone surveying that is aimed at mapping and increasing our understanding of the geothermal field extent and structures at Ytri-Vík. This includes delineating and mapping of surface and sub-surface structures, such as bedrock, dikes, faults, fracture systems, visible water springs, or off-flows, to aid the understanding of geothermal water flow paths in relation to the mapped structural patterns and the underlying geothermal system.

Ytri-Vík is located within the Tröllaskagi structural block, just south of the presently active rift propagation system of the Tjörnes Fracture Zone (TFZ) that transfers spreading and rift extensions from the Kolbeinsey Ridge to the Northern Volcanic Zone (e.g., *Einarsson & Björnsson, 1979; Einarsson, 2008*) (Fig. 1). This distinct right-lateral transform system consists of three parallel WNW-ESE aligned seismic zones, the Grimsey Volcanic Zone, the Husavík-Flatey Fault system (HFF), and the Dalvík lineament (e.g., *Rögnvaldsson, 2000; Einarsson, 2008*). The TFZ offsets most of the extension in the region and has a high level of seismicity along its offshore segments (*Einarsson, 1976; 1991; 2008*). Onshore, the Dalvík lineament has shown little seismic activity but still shows segments of a broad zone across Tröllaskagi and Eyjafjördur that adjusts for extensional processes within the northern segment of Eyjafjördur (Fig. 1). Numerous low-enthalpy sites and boreholes reflect active opening processes in the fjord within a structurally complex region. Ytri-Vík is located within that broad lineament zone and 35 km south of the HFF zone within an overall tectonically active and obliquely WNW-ESE opening rift domain. This oblique opening causes clockwise rotations of fault block segments and dike intrusive features adjacent to the HFF strike-slip fault zone that affects a 10 km wide area between the HHF system and the Gil-Látur Line (e.g., *Horst et al., 2018; Young et al., 2020; Hummel et al., 2022*) (Fig. 1).

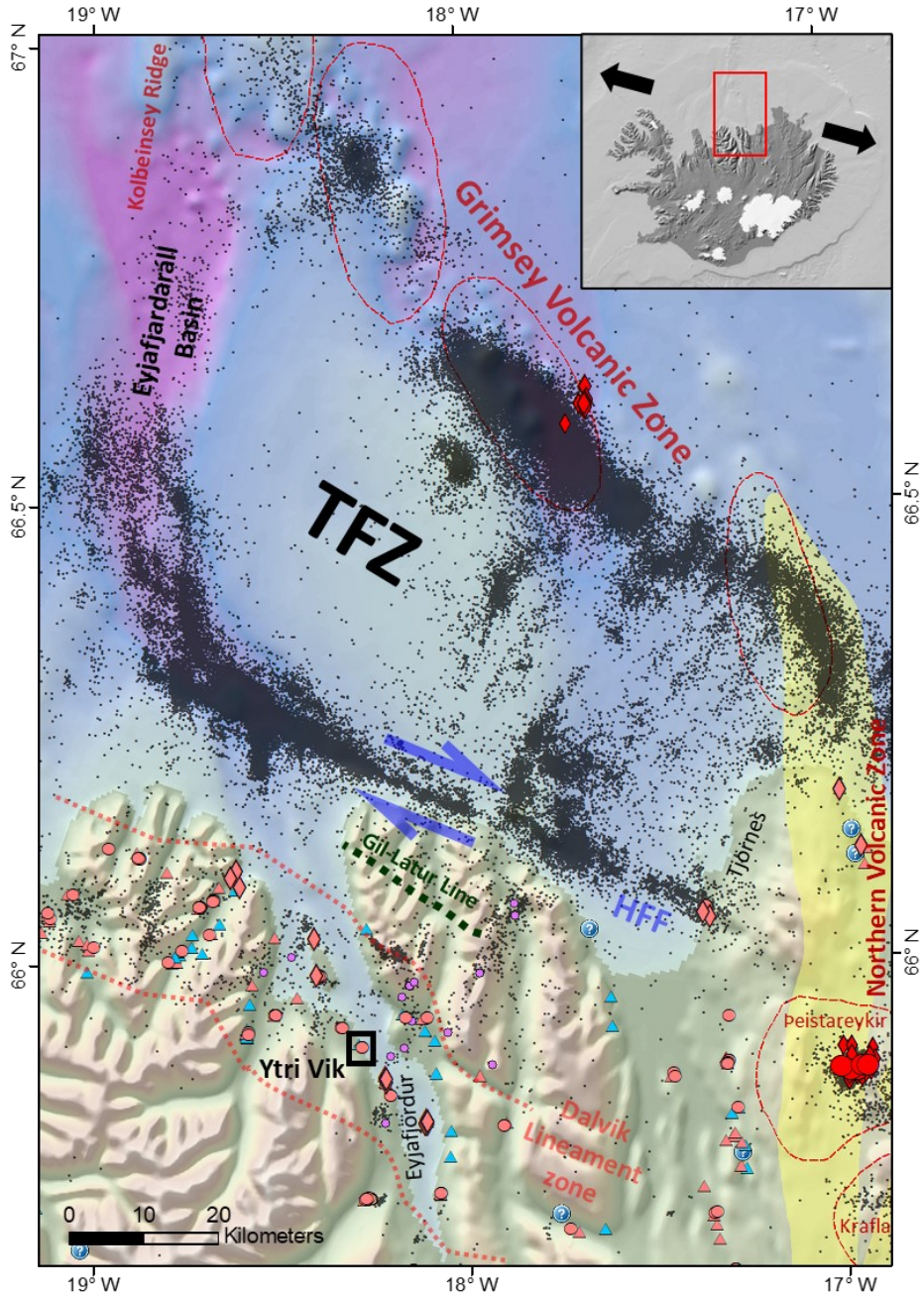

Figure 1: Overview map of the large-scale tectonic elements and volcanic zones of North Iceland, geothermal activity, and field location for Ytri-Vík. Earthquake locations are shown as black dots (*Icelandic Met Office, seismicity database 1995-2022*) and as purple points from *Guðnason et al.* (2020). Tectonic elements and central volcanic systems are labelled on bathymetric features and corresponding seismicity clusters (*Einarsson, 2008; Magnúsdóttir et al., 2015*). The Gil-Látur Line (*Young et al., 1985*) and the DalVík Lineament zone modified after *Einarsson* (2008) are marked on the map. Geothermal manifestations are shown for different temperatures, > 100°C (red), <100°C (light red), and <25°C (light blue). Diamond shapes indicate offshore or nearshore sites, circles for boreholes, triangles for onshore sites, and question marks for geothermal sites that are uncertain. Abbreviation: HFF – Húsavík-Flatey Fault; TFZ – Tjörnes Fractures Zone.

Block rotations increase closer to the HFF system, causing a complex pattern of kilometer-scale crustal blocks and left-lateral internal deformation zones to accommodate increased shearing closer to the right-lateral shearing transform zone (e.g., *Horst et al., 2018; Hummel et al., 2022*).

Further away to the north from the HFF system, large-scale lineaments form NE-SW striking block rotation fault zones, seen as broad bands of NE-SW striking earthquake clusters (Fig. 1), with a left-lateral shearing direction to accommodate the oblique extension of the rift. These processes have been well studied for the HFF system and its adjacent areas, but not for the Dalvík lineament zone, which has no clear offset but appears to be segmented with several geothermal systems, indicating fractured and geothermal water conduits. Ytri-Vík is one of these geothermal systems along the western shore of Eyjafjördur. It is one piece of the puzzle to understand better the Dalvík lineament system and its connection to geothermal up-flow within the Eyjafjördur region.

2. RESEARCH AND DATA

Over the years, considerable research has been carried out for Ytri-Vík and adjacent areas in connection to geothermal exploration (e.g., *Flóvenz & Smárason, 1997; Smárason et al., 2014*). This includes geological and structural field mapping (*Aronson & Sæmundsson, 1975; Brynjólfsson & Hjartarson, 2007; Blischke et al., 2021*), age dating (*Aronson & Sæmundsson, 1975*), and borehole image log analysis work (*Blischke et al., 2017; Gautason & Árnadóttir, 2017*) (Fig. 2). Data sets that address surface and subsurface structures and processes were combined into a composite data analysis database.

2.1 Subsurface data

Magnetic surveying, seismicity, and borehole image log data analysis provided crucial input regarding subsurface locations of intrusions and fault-fracture systems in and around the Ytri-Vík field area.

2.1.1 Magnetic surveying

Total magnetic field surveying has been applied in low-enthalpy geothermal exploration in Iceland to map dike features that are linked to fault zones covered by bedrock or sediment strata with little or no traces visible on the surface (e.g., *Jónsson et al., 1991; Hersir & Björnsson, 1991*). Two total magnetic field surveys were conducted for the Ytri-Vík area in 2017 (*Vilhjálmsson & Tryggvason, 2017*) and in 2022 (Fig. 2).

The 2017 magnetic survey was conducted with the proton precession magnetometer (GSM-19T) on land and near-shore with a line spacing between 25m to 50m (*Vilhjálmsson & Tryggvason, 2017*) (Fig. 2). The survey was focused at Ytri-Vík´s dike exposure along the shoreline that resulted in strong anomalies that overall trend N-S to NNE-SSW and clear internal segmentation (*Vilhjálmsson & Tryggvason, 2017*). A low-intensity anomaly just west of the primary dike system correlates to the bedrock that the intrusive complex cuts through. A fault zone just west of the primary dike is exposed at the shoreline with indications of left-handed fracture movements as part of a dike-parallel fault zone that is down-thrown to the west from the intrusion (*Blischke et al., 2021*) (Fig. 3).

The 2022 magnetic survey was conducted with a MagArrow-mounted DJI Matrice 600 Pro drone (Fig. 2), flown at a 50m constant flight height above ground. The spacing of the primary flight path was held at approximately 50m in a WNW to ESE-oriented direction. The results of the 2022 survey, presented here, are preliminary. The overall N-S orientation and southern extent of the primary dike intrusive system were confirmed by field observations. Magnetic polarity was mapped in the study area as well, as the bedrock lavas stack indicates a polarity reversal that was mapped by *Brynjólfsson and Hjartarson* (2007). The lower lava series at Ytri-Vík has a reverse magnetic polarity of Mid-Miocene age (>11 million years) that is overlain by lava flows of Late Miocene age (11 to 5.3 million years) and has a normal polarity (Fig. 3). All dikes measured in the study area have normal magnetic polarity. The lava exposures near the dikes show variable magnetic polarity, from neutral (neither normal nor reverse) to weakly normal within an overall reverse polarity lava domain along the shoreline and the Mid-Miocene lava series.

The primary dike system is up to 500m wide and consists of a series of 1-20-meter-wide dike segments that are well visible along the shoreline. Most of the onshore part of the dike system is buried further up the slope of Kötlufjall mountain (Fig. 3). Less magnetically intense anomalies can be seen west of the main dike system that is more segmented, has less width (<10m), and variable strike directions between N-S and NNW-SSE.

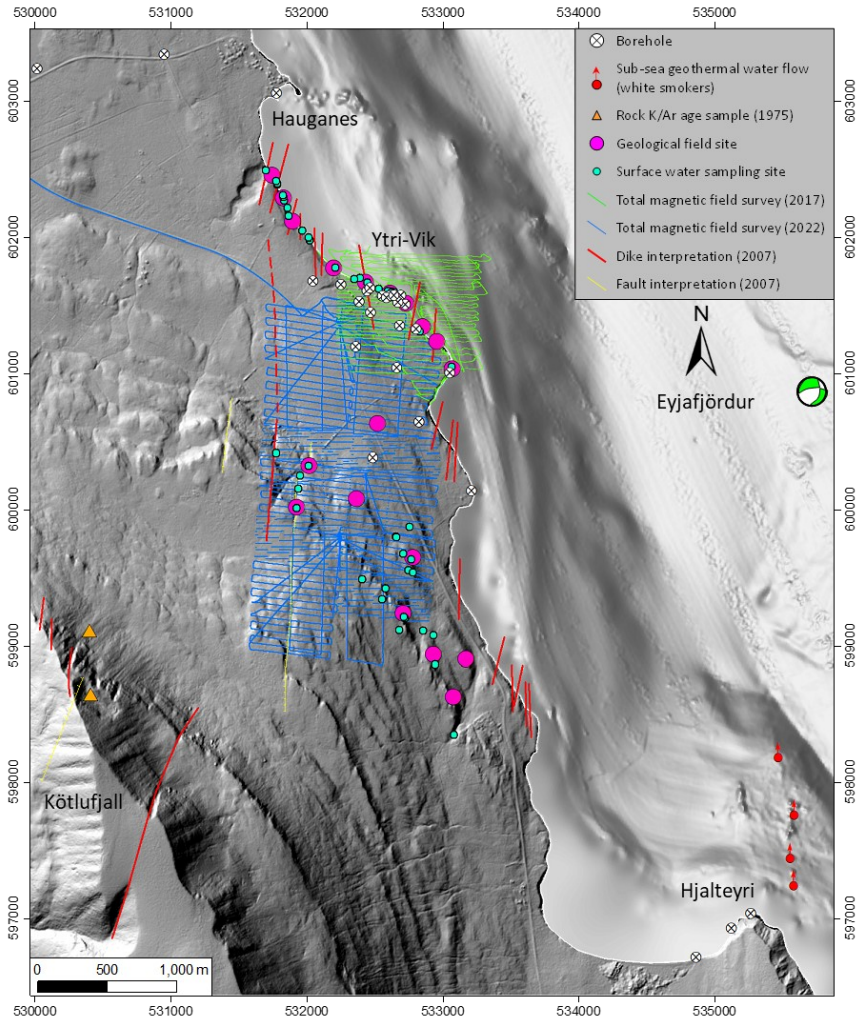

Figure 2: Data location map of magnetic surveys at Ytri-Vík in 2017 (*Vilhjálmsson & Tryggvason, 2017*) and 2022. Boreholes, geological field sites, water sampling locations, and age data points are shown (*Aronson & Sæmundsson, 1975*). Fault lines and dike locations are from field mapping by *Brynjólfsson and Hjartarson* (2007). The shaded topography data is from the DEM2016, and bathymetry data is from *Hjartarson et al.* (2017), including the locations of subsea geothermal water flow and white smokers. An oblique-slip fault plane solution of a mid-Eyjafjördur earthquake at 10 km depth is shown (*Guðnason et al., 2020*).

2.1.2 Subsurface fracturing & stress field orientations

Stress-field analysis was conducted from earthquake data (*Flóvenz & Smárason, 1997; Guðnason et al., 2020*) and borehole data (*Blischke et al., 2017, 2021; Árnadóttir et al., 2019; Gautason et al., 2021; Þorsteinsdóttir et al., 2022*). They were summarized to observe changes in orientations for Ytri-Vík and areas further north in Eyjafjördur (Birnunesborgir) (Figs. 3 & 4).

The closest earthquake and fault plane solution analysis to Ytri-Vík are at Ytri-Vík and at Birnunesborgir (*Flóvenz & Smárason, 1997*), and approximately 2 km offshore, in the center of the Eyjafjörður fjord (Fig. 3). The onshore fault-plane solution indicate NW-SE to N-S oriented faults, whereas the offshore records indicates oblique-slip left-lateral movement due west from an E-W striking plane at an approximate depth of 10 km (*Guðnason et al., 2020*). This demonstrates that structures within Eyjafjördur are still actively moving within an obliquely opening extensional graben within the deepest part of Eyjafjördur. This graben structure can be projected into the Hjalteyri geothermal field and offshore geothermal water springs and white smokers (Fig. 2). These structures indicate that the geothermal system at Hjalteyri is on an active rift belt that extends deep (8–12 km) into the earth's crust, further supported by deep earthquake activity beneath Hjalteyri. Calculated fault plane solutions of earthquakes indicate that seismic activity is related to various movements from strike-slip and oblique-slip to normal faulting, with left-lateral evasive movement in northern segments of Eyjafjördur to normal and oblique-slip deeper into the fjord (*Guðnason et al., 2020*).

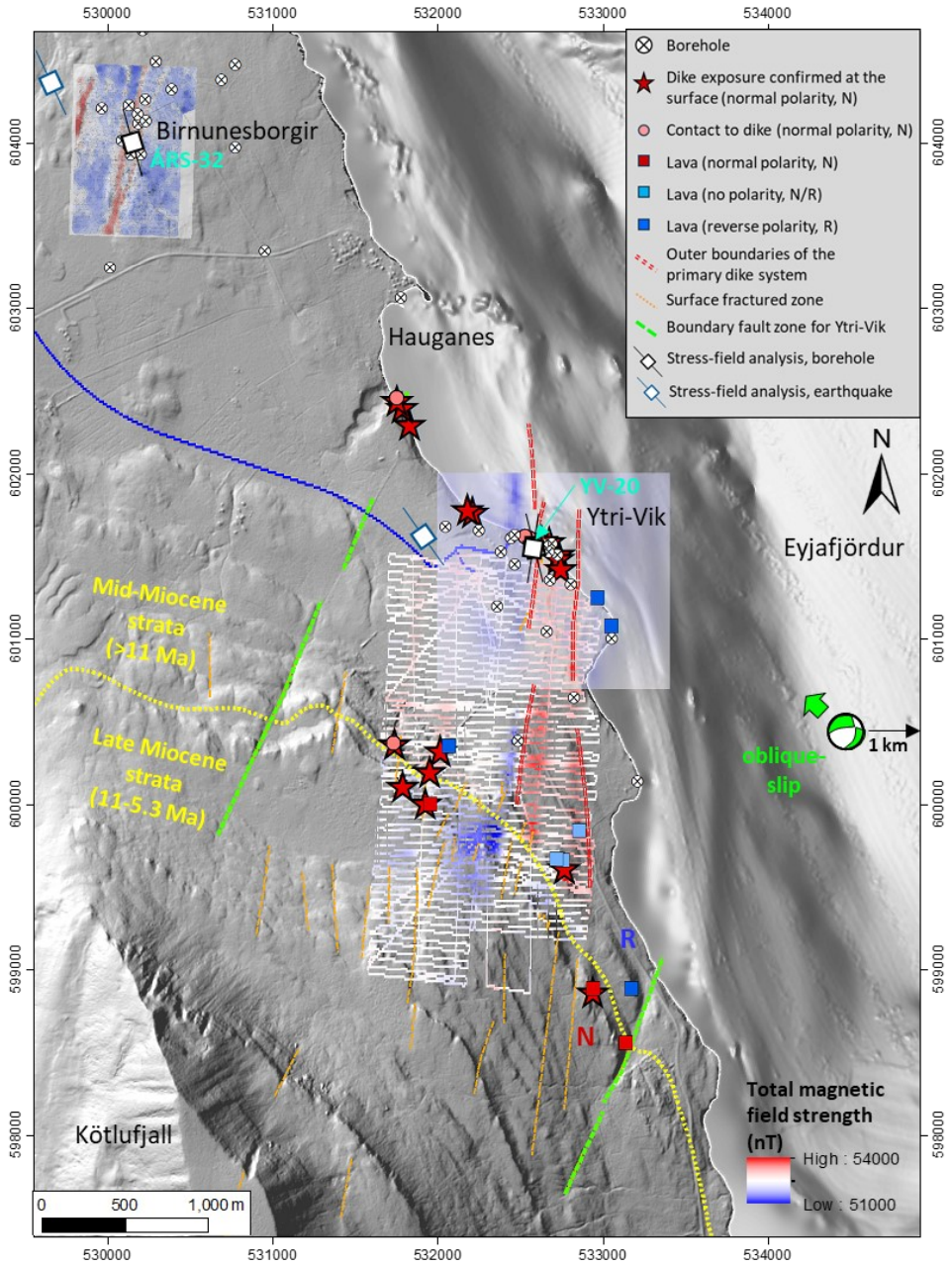

Figure 3: Magnetic data at Ytri-Vík (*Vilhjálmsson & Tryggvason, 2017*) and the line data plot of the 2022 raw data (*this study*) are shown as two main directions of total magnetic field strength anomalies. Fracture zones and dike observations and trends from field work are compared to fracture zone trend directions and the Ytri-Vík boundary fault zones that are based on the elevation model (*Blischke et al., 2021; this study*). The dike series are shown with the highest total magnetic field strength (red color), which cut older bedrock with lower total magnetic field strength (blue color). The primary Ytri-Vík dike complex shows widening to the south, where it terminates. Included is the stratigraphic magnetic polarity subdivision C5n.2n between the Mid- and Late Miocene (*Brynjólfsson & Hjartarson, 2007*). Stress field analysis points are shown for earthquakes (*Flóvenz & Smárason, 1997; Guðnason et al., 2020*) and boreholes ÁRS-32 (*Blischke et al., 2017*) and YV-20.

Borehole image logging and structural analysis are available for borehole ÁRS-32 at Birnunesborgir (*Blischke et al., 2017*), boreholes HJ-18, 19, and 21 at Hjalteyri (*Árnadóttir et al., 2019; Þorsteinsdóttir et al., 2022*), and one borehole, YV-20, at Ytri-Vík (*Gautason et al., 2021*). The analysis for borehole YV-20 shows three dominating fracture set directions: (1) NNW-SSE fracture sets that primarily dip due west; (2) a NNE-SSW striking fracture set, dipping due ESE; and (3) near N-S striking and dike contact parallel fracture sets that steeply dip to the east (Fig. 4). The borehole image analysis of borehole ÁRS-32 at Birnunesborgir (*Blischke et al., 2017*) showed two dominant fracture set directions; the primary open fracture set strikes N-S to NNW-SSE, while the secondary fracture set strikes NNE-SSW, which is parallel to the dike system at Birnunesborgir (Figs. 3 & 4).

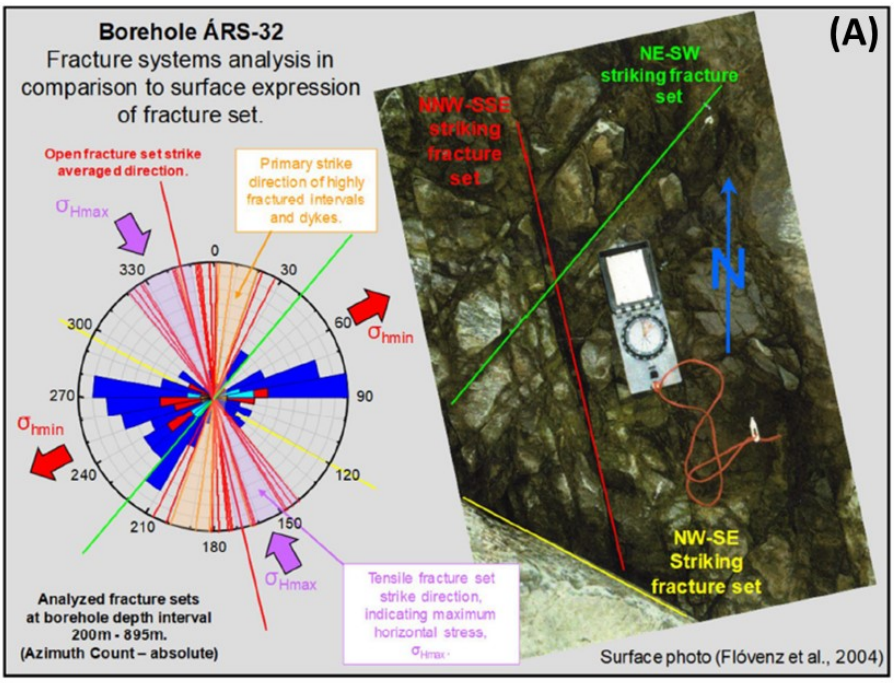

(B) Borehole YV-20, fracture set summary, Modified after *Gautason & Árnadóttir* (2017)

Depth (m)	Q (L/s)	T (°C)	Acoustic image analysis	Wulff-plot (upper hemisphere)
46	0.2	35.5	Open NNW-SSE / W-dipping fracture set; open NE-SV / NV-dipping fracture set; porous strata	
81	2.6	53.5	Multiple narrow NNW-SSE / W- & E- dipping fracture set; porous strata?	
140	8	67.4	Open NNW-SSE / W-dipping fracture set; open NNE-SSW / E- dipping fracture set	
187-198	> 10-13	75.3	Various fracture trends: NE-SW, SE- dipping fracture sets are the most common; some fractures are dipping at low angles.	
246	> 15	~80	Open N-S / steeply east dipping fracture set at dike contact.	

Figure 4: Borehole image log analysis, primary fracture trends and stress field orientation for boreholes: (A) ÁRS-32 in Birnunesborgir (*Blischke et al., 2017*), and (B) YV-20 in Ytri-Vík (*Gautason et al., 2021*). For borehole locations, see Fig. 3.

The direction of the maximum horizontal stress (σ_{Hmax}) from seismicity (*Flóvenz & Smárason, 1997; Guðnason et al., 2020; Young et al., 2020*) and borehole image analysis data (*Gautason et al., 2021*) suggests structural segmentation of Eyjafjördur due to the variable directions within the fjord that align to strike-slip, oblique-slip and dike extension systems. In borehole ÁRS-32, the direction of the greatest horizontal stress (σ_{Hmax}) is striking NNW-SSE, which is similar to the focal mechanism result from earthquakes along the coast north of Ytri-Vík (*Flóvenz & Smárason, 1997*). Borehole YV-20 at Ytri-Vík indicates an N-S oriented maximum horizontal stress field that fits the N-S aligned dike segments (Fig. 3).

2.2 Surface data

Structural surface mapping included high-resolution digital elevation models (DEM) and aerial photography drone acquisition, structural field mapping, and water chemistry sampling along the shoreline and across the Ytri-Vík field of visible fracture- and fault zones and dike exposures. The new data were superimposed on older aerial images (*Loftmyndir ehf., 2018*).

The Iceland DEM model of 2m-by-2m resolution (National Land Survey of Iceland, 2016) provides data coverage outside the drone coverage (Fig. 5). The shoreline dike exposures were first mapped in 2020. Structures were extrapolated to the flanks of the Kötlufjall mountain for planning the magnetic surveys, surface structure and water sampling work in 2022.

2.2.1 Drone Surveying

Drone surveying was conducted in September 2020 and in August 2022 in good weather conditions using a DJI Matrice 200 with a Zenmuse X4S camera. The flight path was held constant at 100 meters above ground for the 2020 survey and 50 meters for the 2022 survey. The image resolution is 2.8 cm, and the image overlap is between 70-80%.

The processed image coverages were superimposed on the digital elevation model adjusted to sea level. The data was used to view and measure field exposures along inaccessible cliff sites, most often not visible in detail on previous data coverages with a lower resolution (Fig. 5). The 3D image model enabled us to view the area from various angles and connect the structures observed in the field.

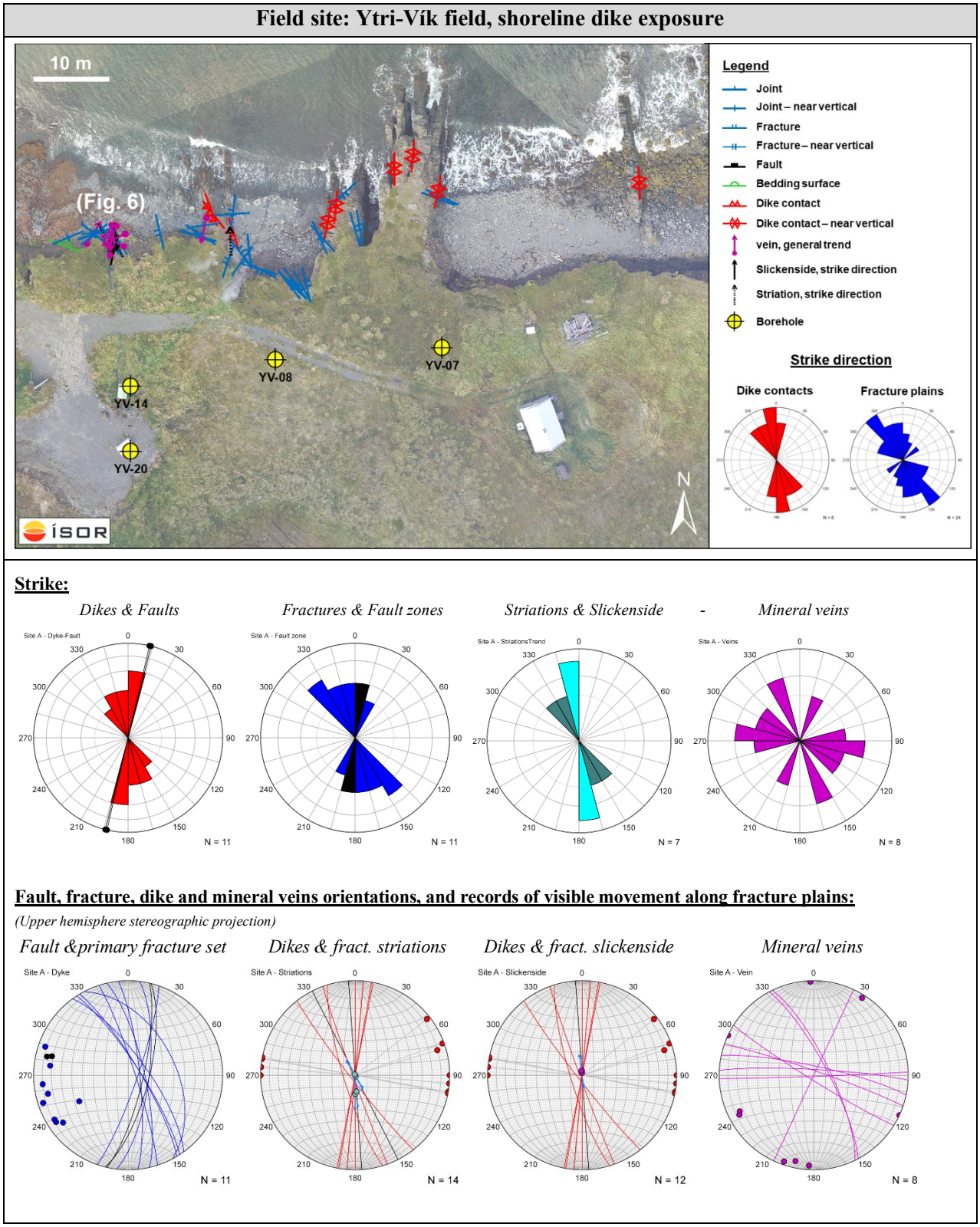

Figure 5: Field site summary for the Ytri-Vík geothermal field as an example of fieldwork conducted for structural surface work (see site locations in Fig. 2).

The much-improved resolution enables us not just to record the general trend of dike features, as has been done traditionally, but also makes it possible to distinguish between dike segments, contacts, or cooling fracture orientations. The elevation model and images were used to differentiate between natural features, human-made objects, and elevation changes, e.g., roads, fences, ditches, or

hedgerows. Other linear features encountered generally have trends consistent with natural structural patterns along the coast and to the SW of the field.

Three dominant trends of dikes and fractures/faults were recorded in a 250–300 m wide outcrop along the coast, i.e., NNW-SSE, N-S and NNE-SSW. These trends correspond well to the borehole image log features of YV-20 (Fig. 4) and magnetic survey data from 2017 (*Vilhjálmsson & Tryggvason, 2017*). The magnetic field strength in Ytri-Vík was measured between 49100 and 58700 nT and aligns well with the trends of faults, dikes, and fractures observed in the drone images (Fig. 5).

2.2.2 Structural field mapping

Structural field data was collected in 2017, 2018, 2020, and 2022 in eighteen field sites, with a focus along the shoreline at Ytri-Vík and onto the NNE flank of the Kötlufjall mountain (Fig. 2). Results from each field site were summarized, see representative example site in Fig. 5, and placed in a structural and geological context. Before visiting the field, the main visible fault lines in the bedrock were drawn based on aerial photographs and a geological map (*Brynjólfsson & Hjartarson, 2007*). Specific focus was set on finding indications of stress-field-related features as kinematic indicators, such as slickenside and striations. Field data was recorded with *FieldMove Clino* digital compass-clinometer; a data capture system that enabled us to account for present-day magnetic declination and to avoid magnetic errors for azimuth readings close to the dikes. We recorded strike, dip, plunge, geological and geothermal descriptions, and magnetic polarity for lavas, dikes and near-dike areas. Magnetic declination was recorded for each day, based on location and timing obtained from the NOAA website (National Centers for Environmental Information at the National Ocean and Atmospheric Administration, 2020), and subtracted from heading readings from the compass. Interpretation and summary of field data were made in Orient 3.13, a spherical projection and data analysis program used for structural geological interpretation (*Vollmer, 2015*). Diagnostic images are shown in an even, spherical and upper hemisphere projection.

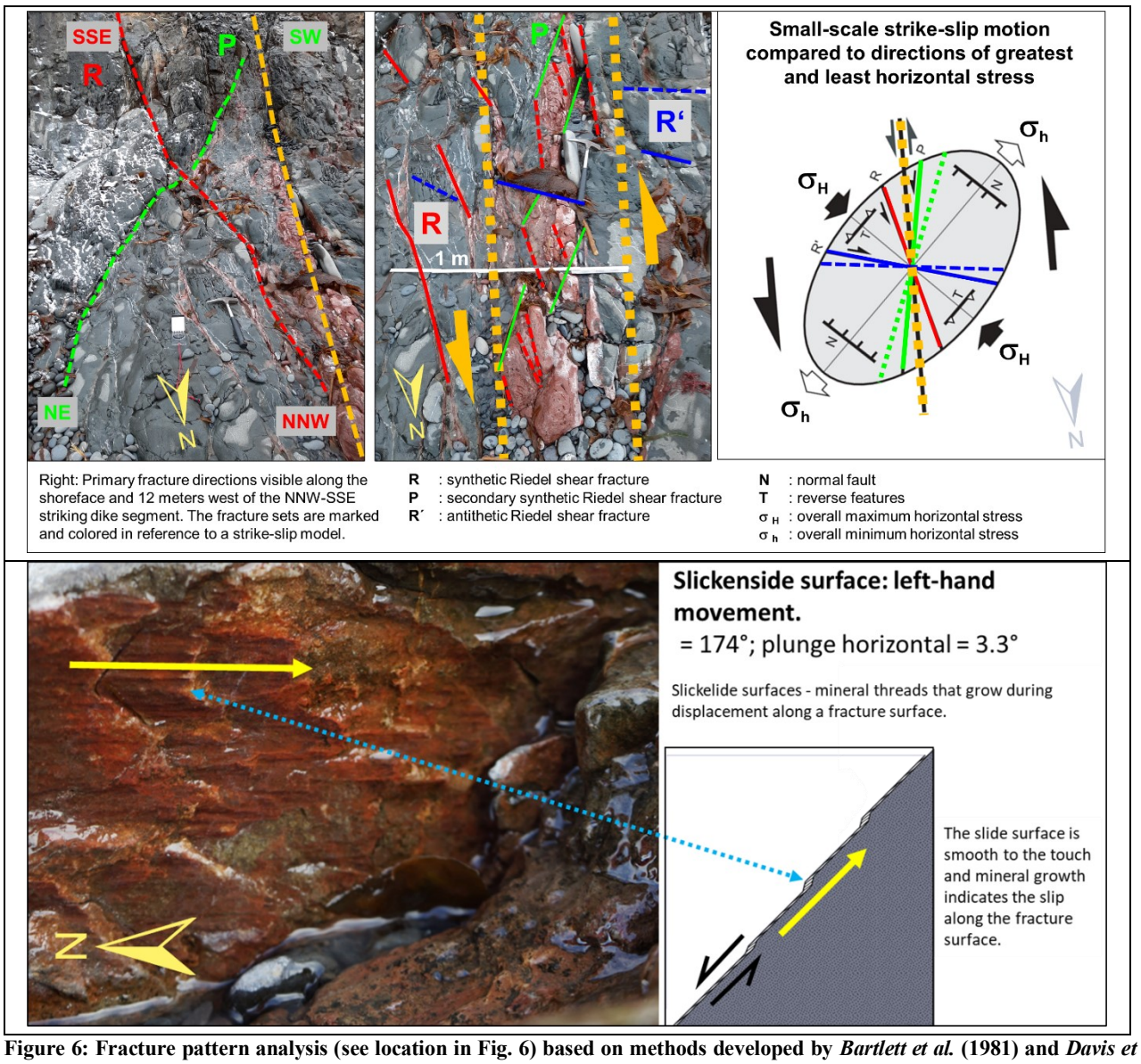

Figure 6: Fracture pattern analysis (see location in Fig. 6) based on methods developed by *Bartlett et al.* (1981) and *Davis et al.* (1999) for strike-slip scenarios, and stress-field estimate for apparent maximum and minimum horizontal stress.

2.2.2.1 Ytri-Vík field example

Structural field measurements from the Ytri-Vík field site show a fault zone on the coast, west of the exposed dike system, that trends NNW-SSE and dips slightly to the WSW (Fig. 5). The primary near-vertical dike segments further to the east trend overall N-S to NNE-SSW. Moderate alteration is visible with oxidized zones and alteration minerals (e.g., calcite) in the primary and open fracture and fault systems that trend NNW-SSE and NE-SW. These directions are also clearly visible in the borehole images (Fig. 4). A smaller and less continuous fracture set trends in a WNW-ESE direction, consisting of primarily tighter and closed fracture segments and mineral veins containing zeolites and clays.

The bedrock close to the dikes is heavily fractured and distorted between the slightly westerly dipping (5°-10°) dike segments with an NNW-SSE trend and the widest near vertical dike segments trending N-S to NNE-SSW. The fractured corridor between the dikes is about 20 to 35 meters wide. Clear deformation and fracture mineralization is visible in the NW-SE and partially WNW-ESE trending fracture sets. Intra-lava sediments are pulled upwards on the east side of the westernmost dike, indicating that that intrusion has pulled it up. In contrast, the fractures and contact on the west side of that intrusion are well open, and geothermal water has circulated through the fractures and joints and altered not just the fractures but several centimeters into the bedrock. Striations along dike parallel fractures are visible, which indicates slight movements in the north-southernly direction. The most open fracture trend is NNW-SSE and dips due west (70°-85°). Present-day strike-slip and oblique-slip fault movements have been recorded within Eyjafjördur in general, north and west of Ytri-Vík, and near DalVík (*Guðnason et al., 2020*).

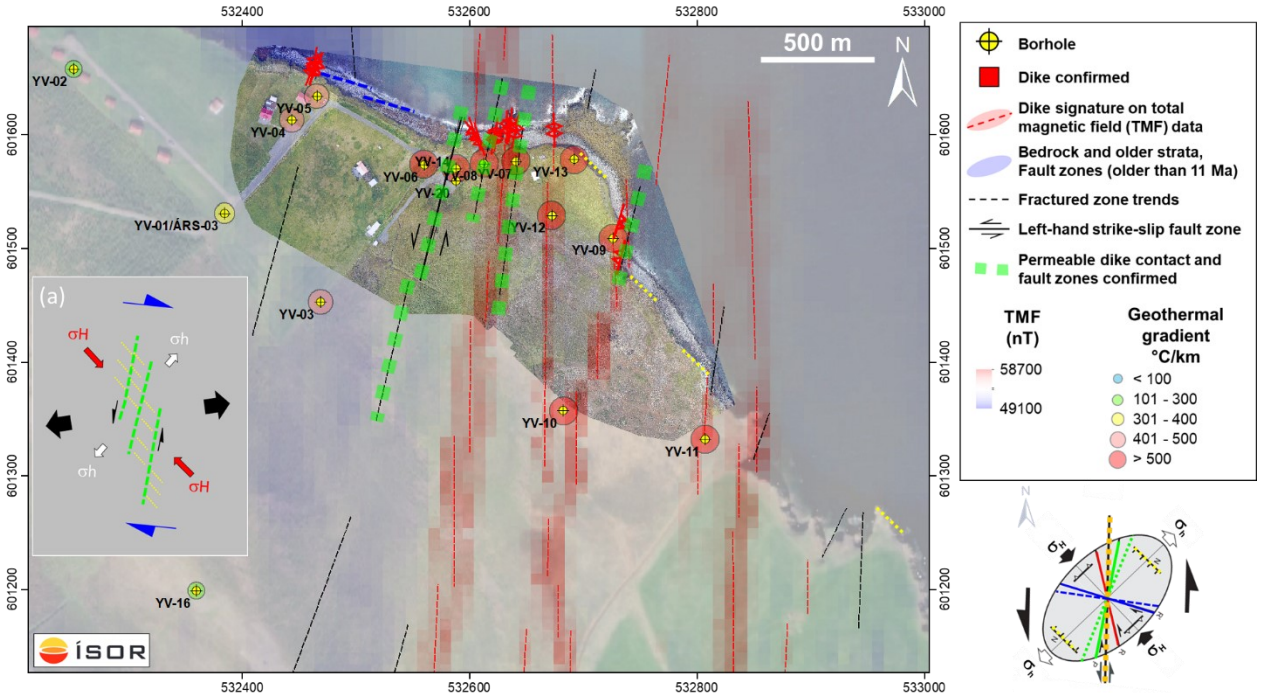

Figure 7: Ytri-Vík field structural geological summary, total magnetic field data (*Vilhjálmsson & Tryggvason, 2017*), drone image and DEM data interpretations. Insert (a) shows the schematic outline of left-lateral bookshelf faulting within an overall right-lateral opening environment based on the structural field observation at Ytri-Vík.

The stress field analysis at the Ytri-Vík site is based on three primary joint and fracture sets (Figs. 5, 6) as a first approach. The fracture pattern model used for describing a strike-slip scenario was developed by *Bartlett et al.* (1981) and *Davis et al.* (1999). The fracture sets at the fault zone indicate that the maximum horizontal stress direction is NW-SE and that the least horizontal stress is oriented in a NE-SW direction, which is similar to known fault plane solutions from earthquakes at Ytri-Vík and north of Ytri-Vík at Birnunesborgir (*Flóvenz & Smárason, 1996*) (Fig. 3). These earthquake-based stress-field orientations are striking about 18° further west than seen on image log data in borehole ÁRS-32 at Birnunesborgir (*Blischke et al., 2017*). There is a difference in maximum horizontal stress orientation to borehole YV-20 with a varying stress field orientation from NNW-SSE to NNE-SSW (average N-S $\sigma_{Hmax.}$ 181° ±10) closer to the dike contact at around 260 meters depth that reflects a greater uncertainty of using the borehole derived stress-fiel data.

The present-day stress-field orientation for $\sigma_{Hmax.}$ of NW-SE is seen in both, the earthquake-derived data and the structural field site analysis within the fault zone just west of the Ytri-Vík dike system (Figs. 3, 6, 7). Horst et al. (2018) described bookshelf faulting within the TFZ that has been described for the area between the Grimsey Volcanic Zone and the HFF marked by NNE-SSW striking earthquake zones (Fig. 1). Insert (a) in figure 7 shows the schematic outline of left-lateral bookshelf faulting within an overall right-lateral opening environment based on the structural field observation at Ytri-Vík with a NW-SE to NNW-SSE normal fault orientation that reflects the present-day extension and coast-parallel faulting. The strike directions of primarily open fracture sets seen in borehole YV-20 are NNW-SSE to near N-S, which indicates open fracture pathways in ENE-WSW and W-E opening directions for the fractured bedrock and the dike contact. The open and near dike fracture sets are in a 20°-40° angle to the coast parallel fractures and general opening direction into Eyjafjördur that reflect both the present-day stress-field response of the area and the dike parallel fracture sets that formed during dike emplacements in Miocene (Fig. 7). Thus, we might see reactivation of older structures with changes in the overall stress-field.

2.2.3 Delineating the southern extension of the dike systems

The primary, overall, north-south striking dike trend is visible in the total field magnetic survey and could be confirmed to its southern extent in the field (Fig. 8). The dike system is connected to a main fault system that strikes NNE-SSW from Ytri-Vík (Fig. 7), accompanied by permeable fault-fracture sets striking NNE-SSW to NW-SE. The 250 to 400 m wide dike system is visible at the shoreline of Ytri-Vík and extends approximately 1 km out to sea and 1.7-2.0 km up the NE slope of the Kötlufjall mountain with a clear total magnetic field strength data response. The last outcropping remains of a 0.5 m thin dike segment were observed 2.6 km at the southeasternmost edge along a fault-fracture zone.

The NNW-SSE striking dike segment that is right next to the west-dipping fault zone, has clear indications of geothermal alteration and the western boundary fault at Ytri-Vík. This is in good correlation with the geothermal gradient distribution from shallow boreholes that only show increased geothermal potential close to the coast (Fig. 7). Little to no comparable alteration indications are observed on the Kötlufjall mountain flank, except slight white mineralization along fracture planes that was apparent for the cliff's sites south of the magnetic anomalies, with water percolating out of fracture zones and runoffs from the cliffs.

Surface water (e.g., creeks, small streams, pools or water-bearing fractures) was measured for temperature, conductivity and pH. Water samples were collected to confirm the field measurements with calibrated lab values. Specifically, conductivity showed a good correlation between the targeted dike system with elevated conductivity values (100-200 µS) on the Kötlufjall mountain flank down to the shoreline (Fig. 8). Conductivity measurements were more challenging along the seashore, as saltwater has high conductivity readings (>20000 µS) and potentially mixes with run-off waters from the land. However, measurements along the coast showed subtle difference between surface water (<100 µS) and potential geothermal water (>200 µS) through fracture systems, excluding conductivity readings (>300 µS) as potential mixing with seawater (>500 µS) (Fig. 8). Along the coast, an area one kilometer further to the NW showed geothermal exploration potential and elevated values in water conductivity that correlated to an area of increased fracturing and dike exposure, in addition to similar recent white secondary mineralization within the fractures, as observed south of the Ytri-Vík dike system. This will need to be investigated in the future.

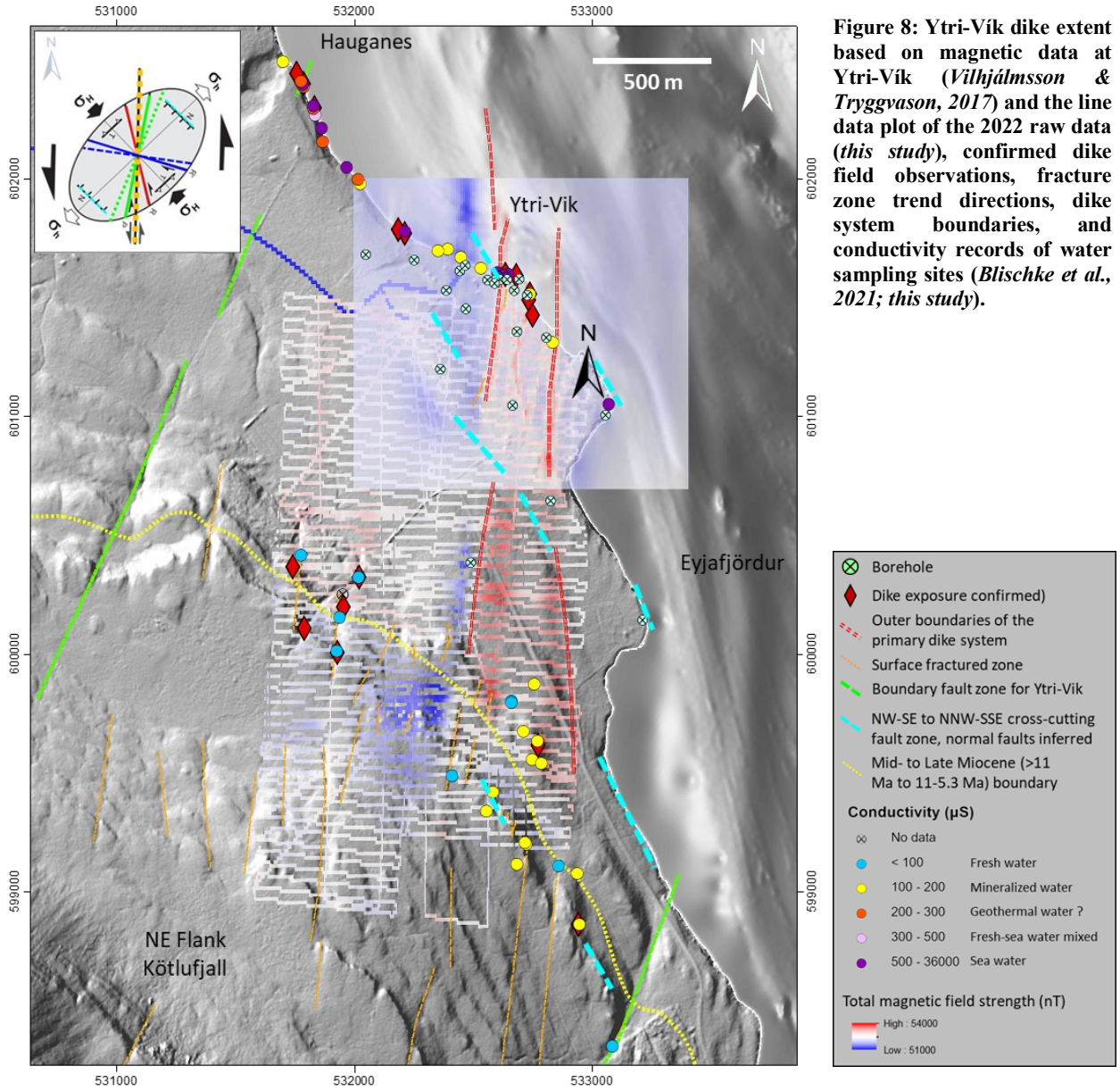

Figure 8: Ytri-Vík dike extent based on magnetic data at Ytri-Vík (*Vilhjálmsson & Tryggvason, 2017*) and the line data plot of the 2022 raw data (*this study*), confirmed dike field observations, fracture zone trend directions, dike system boundaries, and conductivity records of water sampling sites (*Blischke et al., 2021; this study*).

3. STRUCTURAL ANALYSIS AND GEOTHERMAL EXPLORATION

The goal of this project was to carry out structural geology analysis of the surface and subsurface at Ytri-Vík, with the aim of shedding light on the relationship between the geothermal system and the dike system exposed along the coast. Primary questions are the up-flow and the extent of the low-enthalpy system at Ytri-Vík. Therefore, the geological feature extents were mapped and cross-checked with surface water sampling from springs, off-flows, and water trickling from fracture systems at fault zones or dikes (Fig. 8) and placed in the geological context of temporal changes.

3.1 Dike system and stress-field observations

The drone elevation model and structural lineaments based on aerial photographs follow the same directions as the magnetic data, i.e., N-S to NNE-SSW and show a segmentation of six dike segments. The dike segment between boreholes YV-10 and YV-09 may potentially be interpreted as a right-hand en-echelon propagating dike, which would support a left-lateral opening of this dike graben section at the time of emplacement (Fig. 7), which is a well-established emplacement model observed in Iceland, Canary Islands, etc. (e.g., *Clemente et al., 2007; Ruch et al., 2016; Ágústsdóttir et al., 2019*). If this is an observation for Ytri-Vík, then the active stress field during the time of dike emplacement would have been oriented ~N-S for $\sigma_{Hmax.}$ (181° ±10) and ~W-E for $\sigma_{Hmin.}$ Which is based on the image log interpretations of borehole YV-20. The present-day stress-field is recorded in the earthquake data and structural field observations at Ytri-Vík, or the neighboring low-enthalpy geothermal field of Hjalteyri that is located 6km SSE of Ytri-Vík is oriented NW-SE for $\sigma_{Hmax.}$, and reflects the present-day visible structural features on the surface and seismicity. Stress-field orientations can change with time as surrounding tectonic settings change, which can also reflect a change in primarily active fracture release and their orientations. Observed stress release patterns can relate to older structures or depend on the location within the active oblique extensional system, such as the TFZ. The project area has been affected by varying tectonic stresses with changing rotations of larger tectonic blocks and affecting tectonic stresses since the Late Miocene and likely reactivations of initial structures along larger dike systems (e.g., *Horst et al., 2018; Young et al., 2020; Hummel et al., 2022*).

3.2 Geologic and geothermal linkage hypothesis

In the case of Ytri-Vík, the dike intrusive segments strike in general NNE-SSW and N-S, parallel to the NNE-SSW striking fault-fracture zone west of the dike segments. Still, the up-flow of the geothermal system appears to be mainly related to the westernmost NNW-SSE trending dike segment, where the dike contact and associated fractures interlink with the NNE-SSW striking fault-fracture zone, and the highest geothermal gradient was recorded right next to the deepest research borehole YV-20 (Fig. 7). It is also worth noting that the dike system of Ytri-Vík, with its high total magnetic field strength, contrasts with lower field strength readings for confirmed dike segments 500 meters to the west (Fig. 8) that had no indications of alteration, mineralized, or geothermal water traces. The latter dike segment is thus considered to belong to another dike system that does not appear to be hydraulically connected to the underlying geothermal system.

Further sampling of age and petrological composition analysis are necessary to assess for certainty when the various dike systems were formed, as to assess if there is a correlation of geothermal systems to a specific rift and dike emplacement phase. Such additional work would help to unravel the dike emplacement history and make it possible to assign dominant dike strike directions to a specific rift phase. Here it would be interesting to investigate with age analyses if there is a difference in age or composition between the dike systems and if there were several phases of dike emplacement. K-Ar dating of lavas along the coast at Birnunesborgir shows an age of 9.5 ±0.9 and 9.6 ±0.8 million years (*Aronson & Kristján Sæmundsson, 1975*), which is considerably younger than the magnetic period C5r of the Mid-Miocene, which lasted 12.049 – 11.056 million years ago (*Ogg, 2020*), but the bedrock in the area is considered to belong to that period (*Harðardóttir & Hjartarson, 2003; Hjartarson & Sæmundsson, 2014; Young et al., 2020*) (Fig. 9a). The uppermost lavas of the Kötlufjall mountain are 9.1 and 8.7-8.3 million years old according to K-Ar dating (*Aronson & Sæmundsson, 1975*) (Fig. 15). Those lavas have been cut by younger dikes, as can be clearly seen in the landscape west of the mountain.

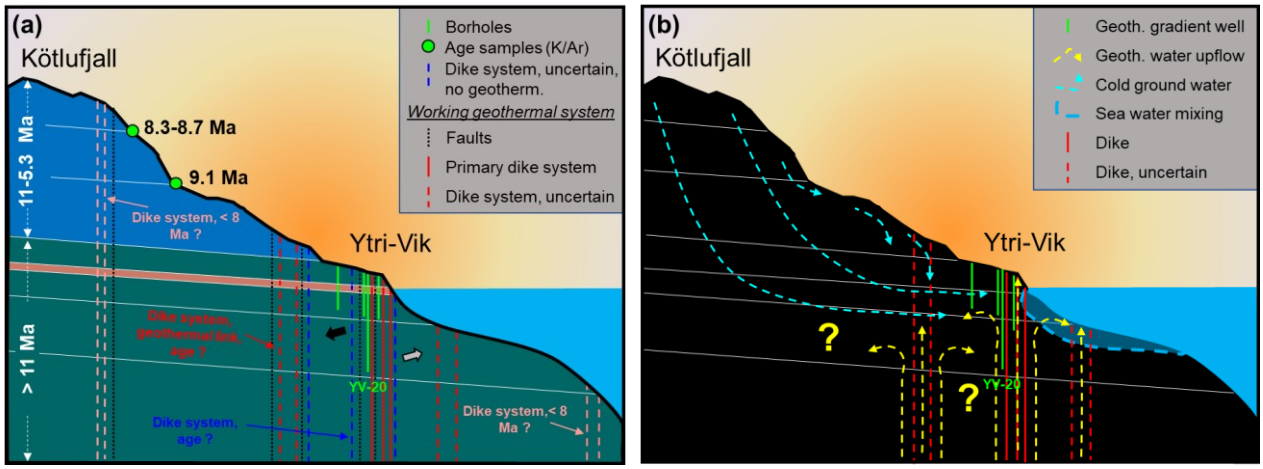

Figure 9: Conceptual model of (a) geology (based on the bedrock map of *Hjartarson & Sæmundsson, 2014*), our observations at Ytri-Vík and our hypothesis that there are two main dike systems, formed at different times or reactivated; (b) possible interactions between groundwater, marine and geothermal systems. Age analyzes of rock layers are from *Aronson and Sæmundsson* (1975). The abbreviation Ma stands for million years.

The geothermal system at Ytri-Vík is most likely related to younger activity that fractured the bedrock, where an older weak zone existed and formed new fault and fracture zones at a similar angle to a previous rifting phase. Thus, the Ytri-Vík dike system connects

well into the geothermal system and conducts geothermal water up to or close to the surface within a tectonic setting that allows the reactivation and interlinking of older and younger, deep reaching structured.

3.4 Geothermal and groundwater systems

The present knowledge of the Ytri-Vík geothermal system prompts some fundamental questions for the area. Warm water springs are mostly found along the coast or valley floors in Eyjafjördur within the DalVík lineament zone (Fig. 1), and not up in the mountains or mountain slopes, where cold water springs are more likely to be found. However, it is known that hot water can be found underneath the mountains, as drilling through the Vadlaheidi tunnel has shown (*Gautason, 2020*). One hypothesis has been discussed as a conceptual model that the high groundwater level builds up enough pressure of the shallow cold-water system from the steep mountains and is high enough to hold an underlying geothermal water system below the surface, except where the land is lowest at the shoreline (Fig. 9b). The conceptual model visualizes a possible interaction between cold water, sea- and geothermal water. It is drawn based on the available data, in particular shallow temperature, and production wells (shallower than 254 m). Boreholes located within the geothermal system clearly show temperature anomalies. If, on the other hand, a cold-water lens lies on top of a geothermal system, lower temperature will be measured in boreholes further up the mountain slope as they do not reach past the cold-water system.

4. CONCLUSION

The goal of this project was to shed light on the connection between the geothermal system at Ytri-Vík and the dike complex that is exposed at the shoreline and access its extent along the coast and to the south onto the Kötlufjall mountain flank and onto its subsea domain. A composite data acquisition and analyses approach was implemented using total magnetic field strength and seismicity data, as well as structure geological and water chemistry data that were superimposed on high resolution topographic and bathymetric data. Surface structural geology was described in relation to the geothermal and groundwater system. The main results of this study are the delineation and confirmation of the 250 m to 400 m wide Ytri-Vík dike complex that trends in a N-S and NNE-SSW direction approximately 1 km out to sea and 2 km – 2.6 km into land from the shoreline and underneath the NE flank of the Kötlufjall mountain. The dike system stands out as a total magnetic field strength anomaly and is connected to a primary fault zone that strikes in a NNE-SSW direction from Ytri-Vík, dipping to the west along the western extent of the dike system. A small dike segment along the western edge of the Ytri-Vík dike complex and at the shoreline strikes in a NNW-SSE direction and is confirmed in borehole YV-20 to be water bearing. The variation in water bearing fault and fracture systems close to the dike complex are possibly connected to several rift phases that were formed during changed stress-field conditions, as at least two fracture sets accommodate geothermal water flow along the western dike contact and boundary. Future research drilling is necessary to confirm the extent and depth of the geothermal system further out to the sea and farther south on land. This research has demonstrated how magnetic surveys, high-resolution drone data, detailed structural geology, and water prospecting can be combined to increase our understanding of low-temperature geothermal systems in Eyjafjördur. Furthermore, this detailed study sheds light on the systematic formation of low-temperature geothermal fields within the Dalvík lineament zone, which requires an understanding of rift formation through time and accompanied changes in stress field. Additional age and petrological sampling and analyses of dike complexes in contrast to the bedrock, and present-day stress field analysis from seismicity data would enable such modeling and understanding of the geothermal systems in Eyjafjördur, and in Neogene areas in Iceland in general.

ACKNOWLEDGMENTS

This work is a part of an ongoing exploration study funded and supported by the Nordurorka Ltd. Utility Company of Akureyri and Eyjafjördur, and the authors would like to thank Nordurorka for allowing publication of their data. We additionally thank Dr. Kirby Young and Dr. Jeffrey A. Karson for their insights on the structural geological setting of Eyjafjördur.

REFERENCES

Arnadóttir, S., Vilhjálmsson, A.M., Egilson, Þ. & Blischke, A. (2019). *Hljóðsjármæling í holu HJ-21 á Hjalteyri*. Íslenskar orkurannsóknir, unnið fyrir Norðurorku, **ÍSOR-2019/081**, 48 s. og 4 viðauki.

Aronson, J.L. & Sæmundsson, K. (1975). Relatively old basalt from structurally high areas in central Iceland. *Earth and Planetary Science Letter*, **28**(1), 83-97. https://doi.org/10.1016/0012-821X(75)90077-1

Ágústsdóttir, T., Winder, T., Woods, J.,White, R. S., Greenfield, T., & Brandsdóttir, B. (2019). Intense seismicity during the 2014-2015 Bárðarbunga-Holuhraun rifting event, Iceland, reveals the nature of dike-induced earthquakes and caldera collapse mechanisms. *Journal of Geophysical Research: Solid Earth*,**124**,8331–8357. https://doi.org/10.1029/2018JB01601

Bartlett, W.L., Friedman, M. & Logan, J.M. (1981). Experimental folding and faulting of rocks under confining pressure Part IX. Wrench faults in limestone layers. *Tectonophysics*, **79**(3–4), 255-277. https://doi.org/10.1016/0040-1951(81)90116-5

Blischke, A., Þorsteinsdóttir, U., Þorbergsson, A., Árnadóttir, S., Vilhjálmsson, A.M. & Gautason, B. (2021). *Jarðhitakerfið við Ytri-Vík. Strúktúrjarðfræðikönnun.* Íslenskar orkurannsóknir, unnið fyrir Norðurorka, **ÍSOR-2021/023**. 49 s.

Blischke, A. Egilson, Þ., Magnússon, I.Þ., Kristinsson, S.G., Flóvenz, Ó.G. & Gautason, B. (2017): *Hola ÁRS-32 á Árskógsströnd - Forrannsóknir, borun og mælingar.* Íslenskar orkurannsóknir, **ÍSOR-2017/091**, 74 s.

Brynjólfsson, S. & Hjartarson, Á (2007). *Árskógsströnd – Jarðfræðikort.*

Clemente, C.S., Amorós, E.B. & Crespo, M.G. (2007). Dike intrusion under shear stress: Effects on magnetic and vesicle fabrics in dikes from rift zones of Tenerife (Canary Islands). *Journal of Structural Geology*, **29**(12), p. 1931-1942. https://doi.org/10.1016/j.jsg.2007.08.005

Davis, G.H., Bump, A.P., Garcia, P.E. & Ahlgren, S.G. (1999). Conjugate Riedel deformation band shear zones. *Journal of Structural Geology*, **22**, 169–190. https://doi.org/10.1016/S0191-8141(99)00140-6

Einarsson, P. (1976). Relative location of earthquakes in the Tjörnes fracture zone. *Vísindafélag Íslendinga*, **Greinar V**, 45–60.

Einarsson, P. & Björnsson, S. (1979). Earthquakes in Iceland. *Jökull*, **29**, 37–43.

Einarsson, P. (1991). Earthquakes and present-day tectonism in Iceland. *Tectonophysics*, **189**, 261–279.

Einarsson, P. (2008). Plate boundaries, rifts and transforms in Iceland. *Jökull*, **58**, 35–58.

Flóvenz, Ó.G. & Smárason, Ó.B. (1997*). Jarðhitaleit á Árskógsströnd 1996*. Orkustofnun, **OS-97002**, 49 s.

Gautason, B., Árnadóttir, S., Tryggvason, H.H. & Hafstað, Þ.H. (2021). *Ytri-Vík - Hola YV-20: Borun, mælingar og jarðlög*. Íslenskar orkurannsóknir, unnið fyrir Norðurorku, **ÍSOR-2021/024**, 38 s. og 2 viðauki.

Gautason, B. (2020). *Áætlun um jarðhitarannsóknir frá 2020 til 2025.* Íslenskar orkurannsóknir, unnið fyrir Norðurorka, **ÍSOR-2020/047**. 24 s.

Gautason, B. & Árnadóttir, S. (2017*). Staðsetning á nýrri vinnsluholu við Ytri-Vík.* Íslenskar orkurannsóknir, unnið fyrir Norðurorku, greinargerð. **ÍSOR-17076**, 7 s.

Guðnason, E.Á, Ágústsdóttir, Þ. & Magnússon, R.L. (2020). *Jarðskjálftavirkni í Eyjafirði 2017-2019*. Íslenskar orkurannsóknir, unnið fyrir Norðurorku. **ÍSOR-2020/015**, 25 s.

Harðardóttir, V.B. & Hjartarson, Á. (2003). *Dalsmynni, geological map*. ISOR Iceland Geosurvey, Reykjavík.

Hersir, G.P. & Björnsson, A. (1991). *Geophysical exploration for geothermal resources. Principles and applications.* UNU-GTP, Iceland, report 15, 94 pp.

Hjartarsson, Á., Erlendsson, Ö. & Gautason, B. (2017). *Hafsbotnsjarðfræði í Eyjafirði Fjölgeislamælingar, hverastrýtur, höggun, skriður, farvegir, jakaför og flök*. Íslenskar orkurannsóknir, unnið fyrir Norðurorku, **ÍSOR-2017/053**, 37 s. og 6 viðauka.

Hjartarsson, Á. & Sæmundsson, K. (2014). *Berggrunnskort af Íslandi, 1:600000*. Íslenskar orkurannsóknir, 1. útgáfa, Reykjavík.

Horst, A., Karsen, J., & Varga, J.A. (2018). Large rotations of crustal blocks in the Tjörnes Fracture Zone of northern Iceland. *Tectonics*, **37**, 1607–1625. https://doi.org/10.1002/2016tc004371

Hummel, N.V., Waag-Swift, S., & Titus, S.J. (2022). Statistical analysis of small faults in rotated blocks of crust near the Húsavík-Flatey transform fault, Northern Iceland. *Journal of Geophysical Research: Solid Earth*, **127**, e2021JB022956. https://doi.org/10.1029/2021JB022956

Jonsson, G., Kristjánsson, L. & Sverrisson, M. (1991). Magnetic surveys of Iceland. *Tectonophysics*, **189**(1-4), 229-247. https://doi.org/10.1016/0040-1951(91)90499-I

Ogg, J.G. (2020). *Geomagnetic polarity time scale*. In: Gradstein, F.M., Ogg, J.G., Schmitz, M. & Ogg, G. (eds.) (2020). *Geologic time scale*. Elsevier, p. 159–192. https://doi.org/10.1016/B978-0-12-824360-2.00005-X

Landmælingar Íslands (2016). *Digital Terrain Model (DTM) of Iceland, 10 m resolution raster dataset, EPSG:3057*. https://www.lmi.is/leyfi-fyrir-gjaldfrjals-gogn/.

Loftmyndir ehf. (2018). *Loftmyndir og myndkort*. https://www.loftmyndir.is

Magnúsdóttir, S., Brandsdóttir, B., Driscoll, N., & Detrick, R. (2015). Postglacial tectonic activity within the Skjálfandadjúp Basin, Tjörnes Fracture Zone, offshore Northern Iceland, based on high resolution seismic stratigraphy. *Marine Geology*, **367**, 159-170. https://doi.org/10.1016/j.margeo.2015.06.004

NOAA (2020). *Magnetic Field Calculators*. Source: https://www.ngdc.noaa.gov/geomag/calculators/magcalc.shtml#declination

Rögnvaldsson, S.T. (2000). *Kortlagning virkra misgengja með smáskjálftamælingum* – yfirlit. Rit Veðurstofu Íslands, Reykjavík, VÍ-R00001-JA01, 15 s. ISBN 9979-878-16-9

Ruch, J., Wang, T., Xu, W., Hensch, M. & Jónsson, S. (2016). Oblique rift opening revealed by reoccurring magma injection in central Iceland. *Nat Commun*, **7**, 12352. https://doi.org/10.1038/nco mms12352

Smárason, Ó.B. et al. (2014). *Árangursrík jarðhitaleit við Ytri-Vík á Árskógsströnd árin 1994 til 1996*. STAPI Jarðfræðistofa, 18 bls, viðauki A og B.

Þorsteinsdóttir, U., Arnadóttir, S. & Blischke, A. (2022). *Hljóðsjármælingí holu HJ-19 á Hjalteyri: Sprungugreiningog mat á spennusviði*. Íslenskar orkurannsóknir, unnið fyrir Norðurorku, greinargerð ÍSOR-22065, 48 s. Og 4 viðauki.

Vilhjálmsson, A.M. & Tryggvason, H. (2017). *Segulmælingar við Ytri-Vík.* Íslenskar orkurannsóknir, unnið fyrir Norðurorku, **ÍSOR-2017/068**, 27 s.

Vollmer, F.W. (2015). Orient 3: a new integrated software program for orientation data analysis, kinematic analysis, spherical projections, and Schmidt plots. *Geological Society of America Abstracts with Programs*, **47**(7), p. 49.

Young, K., Orkan, N., Jancin, M., Sæmundsson, K., & Voight, B. (2020). Major tectonic rotation along an oceanic transform zone, northern Iceland: Evidence from field and paleomagnetic investigations. *Journal of Volcanology and Geothermal Research,* **391**, 106499, p. 25. https://doi.org/10.1016/j.jvolgeores.2018.11.020

Young, K., Jancin, M., Voight, B., & Orkan, N. (1985). Transform deformation of Tertiary rocks along the Tjörnes fracture zone, north central Iceland. *Journal of Geophysical Research*, **90**(B12), 9986–10010. https://doi.org/10.1029/JB090iB12p09986